

# Modelling of the effects of porosity and particle size on the steady-state wave velocity in combustion synthesis

A. K. BHATTACHARYA\*

*Department of Materials Science and Engineering, University of Cincinnati, Cincinnati, OH 45221, USA*

A simple model has been developed for steady-state combustion wave velocity which takes into account the effects of porosity, pore size and powder particle size. This model uses a unit-cell approximation for a characteristic porous compact geometry and also a description of heterogeneous reaction is utilized as an approximation to explicitly include the effect of particle size. Parametric studies indicate that as the porosity increases the combustion propagation rate decreases. It is also inferred that the pore size plays an important role in this behaviour and it can even reverse this trend at high values of pore size. As observed in combustion experiments, the model also correctly predicts the increase in combustion velocity with decreasing particle size.

## 1. Introduction

Starting from the pioneering works of Merzhanov and others [1–3], combustion synthesis of materials is being adopted more and more for the synthesis of advanced ceramics, intermetallics and composites [4, 5]. This process utilizes highly exothermic self-sustaining chemical reaction between two or more species which propagate as a combustion wave through a compacted mixture of reactant powders.

It has been claimed that because of the very high temperatures quickly achieved in such a combustion process, the products are of high purity [6–8] since most of the impurities become volatile at these temperatures. The principal advantage of such a process can be a shorter processing time, a possible reduction in reinforcement–matrix reaction and the elimination of any high-temperature furnace necessary for the conventional fabrication route.

By controlling the important input parameters related to the actual combustion phenomenon, the rate of combustion wave propagation can be controlled and as the controlled reaction front advances through the material, the reactant powder mixture is converted to the desired product. It is therefore important that one tries to understand these processes of wave propagation and its dependence on various important parameters.

So far substantial efforts in the development of combustion or reaction synthesis have been directed towards the experimental aspect of it and it has developed from an empirical art to a rational activity. On the other hand, considerable attention has also been focused on the modelling aspect of the process. The broad spectrum of a typical reaction process includes inherently disparate space and time scales

and realistic analysis of the phenomenon has to include a complete description of the different processes involved with regard to mass, momentum and energy balance for the participating system. Most of the earliest attempts to model such processes have made simplifying assumptions and although they provide us with important guidelines, consistent agreement between these simulations and experimental observations is not usually obtained. Moreover, the number of modelling studies which relate microstructural information to the combustion process is rather limited [9].

There is, however, extensive combustion-related theoretical research on the propagation of the reaction front in reacting systems without including important microstructural parameters like porosity, particle size etc. As the combustion products are formed, one of the most important factors that determine the nature of combustion is the velocity of the propagating wave of the reaction front. The governing system of partial differential equations representing mass and energy balance, together with appropriate initial and boundary conditions, constitute a mathematical model for the behaviour of such a reaction system. Generally the analyses of these systems of non-linear equations prevent analytical solutions from being obtained in a closed form except in certain simplified situations. With the simplification that the reaction zone width is narrow compared to the heating zone, various authors [10, 11] have derived the expression for adiabatic velocity  $V_a$  for steady-state combustion. Although these analyses provide important qualitative correlations between adiabatic temperature, wave velocity, heat of formation, activation energy etc, they do not take into account the effect of porosity or the powder

\* Present address: Material Science and Technology Division, Los Alamos National Laboratory, Los Alamos, NM 87545, USA.

particle size in the compacted material. The objective of the present work is to develop a treatment for steady-state combustion wave velocity by taking into account the effect of these important microstructure parameters. As we will see subsequently, these two parameters have significant effect on the combustion process which have been seen in the experimental work of various authors [7, 12, 13].

## 2. Model formulation

Without any regard to the powder particle size and shape or porosity of the compact, the governing equation (one-dimensional case) for heat transfer in the combusting material is

$$\rho c_p \frac{\partial T}{\partial t} = \frac{\partial}{\partial x} \left( k \frac{\partial T}{\partial x} \right) + \rho Q \phi(T, \eta) \quad (1)$$

where  $\rho$  is the density of the compact,  $c_p$  is its specific heat capacity,  $k$  the coefficient of thermal conductivity,  $Q$  the heat release per unit mass of reacting material,  $\eta$  the reacted fraction and  $\phi$  the kinetic heat release term. The term  $\eta$  is dependent on reaction concentration  $c$ . The relation between  $c$  and temperature  $T$  at each point of the combustion wave is generally unknown but it can be obtained by solving appropriate equations incorporating species concentration. Based on the above basic equation we next develop how the effects of porosity and particle size can be incorporated.

### 2.1. Effect of porosity

First of all we look at how the effect of porosity  $p$  can be modelled and included in the governing Equation 1. The porosity will have the strongest effect on the density  $\rho$  and the coefficient of thermal conductivity  $k$ . The density at a porosity  $p$  is given by  $\rho = \rho_s (1 - p)$ , where  $\rho_s$  is the solid density at zero porosity. To look at the effect of porosity on the thermal conductivity, we make a simplifying assumption that the mixed powder particles have diameters not too far from each other, so that we could approximate an average diameter  $d = \sum d_i / \sum i$ , where  $d_i$  is the average diameter species  $i$ . For making the modelling tractable we shall also assume here that after cold compaction, the

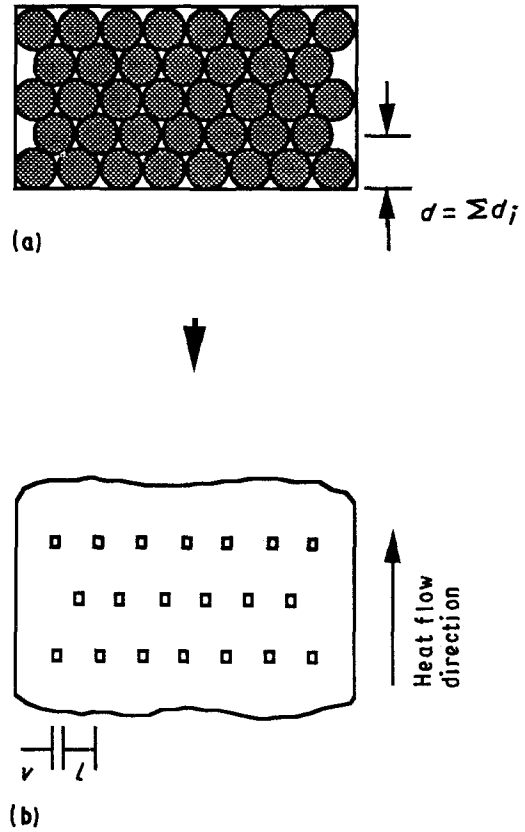


Figure 1 Transformed model representation in terms of solid and isolated regular arrays of closed pores.

ductivity  $k$  in the combustion synthesis problem is almost always considered as that of a solid mass. In reality, however, the transport of heat through the porous compact will occur by a combination of conduction, convection and radiation. Their cumulative effect can be represented as an overall thermal conductivity  $k_e$ . The problem of finding an overall thermal conductivity in a compacted powder mass has been recently discussed [16] following a treatment similar to that of Zumbrunnen *et al.* [14]. Here, the geometry of the compact has been modelled as in Fig. 1a and b with the simplification that all pores have a single characteristic size  $v$  and that all pores are evenly spaced by a distance  $l$  perpendicular to the heat flow direction. The effective thermal conductivity can then be expressed as [16]

$$k_e = \left[ \chi + \Gamma \left( 1 + \frac{1}{\delta} \right) + 1 \right] / \left[ \frac{1}{k_s} \left( \frac{\Gamma}{\delta} + \chi \right) + \frac{1 + \Gamma}{[v h_r + (k_p/\mu)]} \right] \quad (2)$$

where

$$\delta = \frac{v}{l} = \frac{p^{1/3}}{1 - p^{1/3}} \quad (3)$$

$$\chi = (1 + \delta) \left[ \left( \frac{2 + \delta}{1 + \delta} \right) \ln(1 + \delta) + 1 \right] / [\delta \ln(1 + \delta)] \quad (4)$$

powder particles are stacked up as shown in Fig. 1a which shows that the particles are squeezed in a regular fashion.

There is a considerable amount of work on the determination of effective thermal conductivity in a porous medium [14, 15]. At present the thermal con-

$$\Gamma = 1 + \frac{1}{\ln [1 + (1/\delta)]} \quad (5)$$

Here,  $h_r$  is the effective heat transfer coefficient for radiation across the pores and is given as

$$h_r = 4 \varepsilon \sigma \bar{T}^3 \quad (6)$$

where  $\bar{T}$  is the average temperature of the pore surface;  $k_s$  is the average thermal conductivity of the unreacted powders and  $k_p$  the thermal conductivity of the fluid in the pores, which is assumed to be air for the present treatment.  $\varepsilon$  and  $\sigma$  are the emissivity of the pore surface and Planck's constant, respectively.  $\mu$  is an adjustable parameter that relates the conduction across the pores to the local conductivity of the solid. Equation 2 can be rewritten as

$$\frac{k_c}{k_s} = \left[ \chi + \Gamma \left( 1 + \frac{1}{\delta} \right) + 1 \right] / \left( \chi + \frac{\Gamma}{\delta} + \frac{1 + \Gamma}{\left\{ \Omega [T_b^3(\rho)] / [T_b^3(\rho_s)] + (1/\mu) (k_p/k_s) \right\}} \right) \quad (7)$$

where  $\Omega = 4v\varepsilon\sigma T_b^3(\rho_s)/k_s$  is a parameter containing pore size and  $T_b(\rho_s)$  is the adiabatic combustion temperature in the material with zero porosity;  $\mu$  is the parameter that has been determined to be 0.5 on average for a typical material to give best agreement between experimental and theoretical results [14]. It has been assumed here that the average temperature  $\bar{T}$  at the pore equals the adiabatic temperature  $T_b(\rho)$  of reaction. In reality  $\Omega$  as a parameter signifies the relative importance between the thermal conductivity across pores due to radiation and the thermal conductivity of the solid powder. Equation 7 is the desired relationship which relates the overall conductivity with porosity in the compacted mass. As expected, the left-hand side of the equation becomes unity when the porosity becomes zero.

## 2.2. Effect of pore size and porosity

It is generally observed that the green density (related to porosity) increases with increasing particle size because this leads to more particle movement and a more desirable distribution of stresses within the mass, leading to greater deformation. During compaction and densification, one of the basic changes that takes place is the closing off of porosity so as to form isolated pores. Once pores become isolated it is extremely difficult to have solid materials fill in that space, and reducing the particle size will only promote such entrapment. Thus, under an applied pressure, a smaller particle size results in a lower green density and leads to a higher porosity. Clearly, in this case the higher porosity in the green compact is due to a greater number of pores in spite of the fact that the average size of these pores will be smaller in compacts made of smaller particles. With these observations, the pore size  $v$  and porosity  $p$  can be related as [17]

$$p(P) = p(0) \operatorname{erfc} \left( \log \frac{v(0)}{v(P)} \right) \quad (8)$$

where  $p(P)$  is the porosity at pressure  $P$ ,  $p(0)$  is the porosity at zero applied pressure,  $v(0)$  is the largest pore size at zero applied pressure and  $v(P)$  is the largest pore size at pressure  $P$ .

In the present analysis we will consider the pores to be of uniform size with or without pressure. We assume that at zero applied pressure the powder particles are stacked up in a simple manner as shown

in Fig. 2. This gives rise to a pore size and porosity

$$\begin{aligned} p(0) &\approx 0.476 \\ v(0) &\approx 0.46 d \end{aligned} \quad (9)$$

Thus, Equation 8 becomes

$$p(P) = 0.476 \operatorname{erfc} \left( \log \frac{0.46 d}{v(P)} \right) \quad (10)$$

This expression relates the pore size, particle diameter and porosity.

## 2.3. Effect of powder particle diameter

Apart from influencing the pore size in the compacted material as discussed, the average particle diameter  $d$  is expected to have a fundamental effect on the combustion process itself by affecting the kinetics of chemical reaction. In the theoretical analysis of solid-state combustion synthesis, the reaction consisting of the interaction of the product layer and the initial unreacted material is not usually taken into account [18–20]. However, it can be assumed that these processes can be indirectly taken into account by appropriate kinetic laws. Apart from a number of experimental observations, it has been seen [21] that the average particle diameter  $d$  very strongly affects the kinetic function  $\phi$  in Equation 1 in terms of the order of reaction.

In the following treatment an interaction reaction is considered to take place between two reacting particles forming a product layer of thickness  $\Delta$ . Considering a power-law type reaction, the variation of  $\Delta$  can be given as [21, 22]

$$\frac{d\Delta}{dt} = \frac{k_0 \exp(-E/RT)}{\Delta^n} \quad (11)$$

where  $n$  is a kinetic parameter characterizing the type of reaction, and  $k_0$  is a pre-exponential factor. Here, although the above description is to treat the system as heterogeneous, we assume that the medium behaves as homogeneous in the thermal sense and thus the above description can be used in the present case as an approximation. The volumetric rate of heat release  $\phi$  in Equation 1 can then be given as

$$\phi = (1 - \eta)^a \frac{k_0 \exp(-E/RT)}{r_0^{n+1} \eta^n} \quad (12)$$

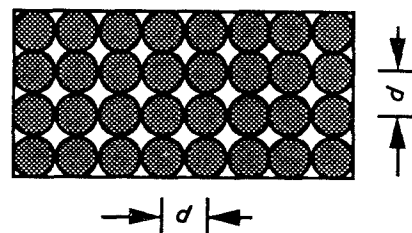


Figure 2 Simple stacking of powder particles without any applied pressure  $P$ .

where  $\eta = \Delta/r_0$  is the reacted fraction,  $r_0$  is the average radius of the particles and  $a$  is a constant factor related to the geometry of the particles. For our subsequent discussions we will consider only the linear case signified by  $n = 0$ , i.e. zero-order reaction. Thus Equation 1 can be finally expressed as

$$\rho c_p \frac{\partial T}{\partial t} = \frac{\partial}{\partial x} \left( k_e \frac{\partial T}{\partial x} \right) + 2\rho Q \frac{(1-\eta)^a}{d} k_0 \exp\left(-\frac{E}{RT}\right) \quad (13)$$

#### 2.4. Steady-state combustion velocity

For the purpose of looking at the behaviour of the combustion front, we shall consider that the heat generation rate in the combustion wave, due to a very strong temperature dependence of the reaction rate, can be neglected everywhere except in a narrow zone in the vicinity of the combustion front. Under such conditions Equation 13 becomes

$$\frac{d}{dx} \left( k_e \frac{dT}{dx} \right) - c_p G \frac{dT}{dx} + \rho Q \phi(T, c) = 0 \quad (14)$$

where  $c$  is the relative concentration of the reactant and  $G$  is the mass combustion velocity, related to the normal combustion front velocity  $u_n^*$  by

$$G = \rho u_n^* \quad (15)$$

and

$$\begin{aligned} \phi(T, c) &= \frac{2c^a}{d} k_0 \exp\left(-\frac{E}{RT}\right) \\ &\equiv \Phi(c) k_0 \exp\left(-\frac{E}{RT}\right) \end{aligned} \quad (16)$$

Thus the reaction rate function is given as

$$\Phi(c) = \frac{2c^a}{d} \quad (17)$$

Following a treatment similar to that of Merzhanov and Khaikin [18] we obtain an expression for the mass combustion velocity

$$G^2 = \left( \int_0^1 \frac{cdc}{\Phi(c)} \right)^{-1} \frac{\rho k_e R T_b^2}{QE} k_0 \exp\left(-\frac{E}{RT_b}\right) \quad (18)$$

After integration using Equations 15 and 17, we obtain the steady-state normal combustion wave velocity

$$u_n^* = \frac{2k_e T_b^2}{\rho d} \left( \frac{R}{AQE} \right) k_0 \exp\left(-\frac{E}{RT_b}\right) \quad (19)$$

where  $A$  is a constant related to a definite integral of  $c$ .

Although the above equation gives us the steady-state combustion velocity, determination of its absolute value involves some uncertainties due to the presence of the pre-exponential factor  $k_0$ . In what follows next, we shall therefore look at how the combustion wave velocity in a non-dimensional form is affected by the various parameters of interest, particularly the porosity, pore size parameter and the

particle size. It follows from Equation 19 that at two different porosities and particle sizes

$$\begin{aligned} \frac{u_n^*(p_2, \Omega_2, d_2)}{u_n^*(p_1, \Omega_1, d_1)} &= \left[ \frac{k_e(p_2, \Omega_2)}{k_e(p_1, \Omega_1)} \left( \frac{1-p_1}{1-p_2} \right) \right. \\ &\times \left. \left( \frac{T_b(p_2)}{T_b(p_1)} \right)^2 \left( \frac{d_1}{d_2} \right) \right. \\ &\times \left. \frac{\exp[-E/RT_b(p_2)]}{\exp[-E/RT_b(p_1)]} \right]^{1/2} \end{aligned} \quad (20)$$

This form of the equation assumes the same values of  $k_0$ ,  $Q$  and  $E$  for two different compact states and calculates the relative effect of the various parameters on the combustion velocity.

### 3. Results and discussion

In this section we present some of the results predicted by the developed model. For the purpose of calculation we take a specific case of combustion in the Ti-C-Ni(25%) system. The relevant physical properties related to the model for this system are summarized in Table I, where some of these properties have been adopted from Dunmead *et al.* [23]. An average value of  $k_s$  has been considered for an appropriately homogeneous mixture of Ti, C and Ni.

#### 3.1. Effect of porosity and pore size

Fig. 3 represents how the effective thermal conductivity  $k_e$  changes with the porosity of the compact as predicted by Equation 7. The plots are made for four different pore sizes represented by the parameter  $\Omega$ . As

TABLE I Input physical properties of Ti-C-Ni system

|  |  |
|--|--|
| Thermal conductivity of powder material having zero porosity | 45 W m <sup>-1</sup> K <sup>-1</sup>   |
| Adiabatic temperature  | 2494 K                                 |
| Activation energy  | 133 kJ mol <sup>-1</sup>               |
| Pore emissivity  | 1 (black-body radiation)               |
| Thermal conductivity of fluid (air) inside pores             | 0.08 W m <sup>-1</sup> K <sup>-1</sup> |

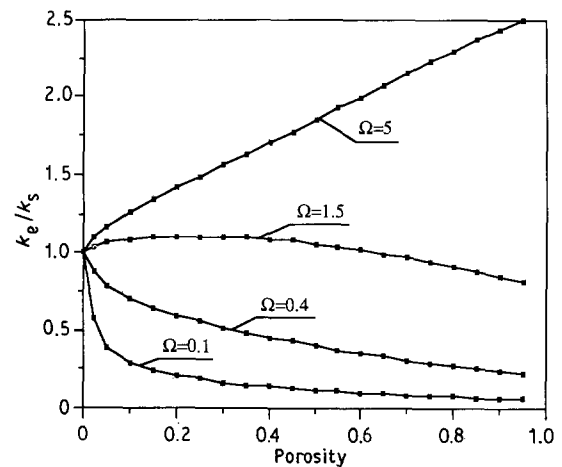


Figure 3 Effect of porosity on the effective conductivity of a porous compact as a function of the dimensionless pore size parameter  $\Omega$ .

indicated in Table I, for the purpose of calculation in this study we assume that the pore surfaces are black although any other emissivity value can be considered, if known for the material. We notice that the effective thermal conductivity of the porous compact is a very strong function of porosity and that it also strongly depends on the size of pores. For a fixed pore size in the small and high ranges of  $\Omega$  values,  $k_e$  monotonically decreases and increases, respectively. In the intermediate level of pore sizes as typically represented by  $\Omega = 1.5$  in Fig. 3, the effective conductivity has a mixed behaviour. With an increase in pore size at the same porosity, the effect of radiation becomes more and more important, thus giving rise to increasing conductivity. At very large pore size, the effective conductivity seems to be exceeding the solid conductivity for all porosity levels. There exists only limited information on the experimental observation of the effect of pore size [24], on conductivity; the measured pore sizes in such cases have also been very small, typically in the range  $10^{-3}$ – $10^{-2}$  mm. Thus, even a meaningful qualitative comparison with the behaviour in Fig. 3 cannot be directly made, but the overall trend clearly indicates that the level of porosity and pore size can have a profound effect on the overall heat transfer characteristics.

In Fig. 4 we show how the porosity and pore size affect the steady-state combustion velocity given by Equation 20. This study has been done without any consideration of the particle size, i.e. the particle size has been kept constant. The other important consideration is to be able to calculate the effect of density or porosity on the adiabatic temperature  $T_b(\rho)$ . Here, due to lack of any direct theoretical information on  $T_b$  versus  $\rho$  without solving the complete boundary-value problem, we resort to some experimental observations [12, 23] on Ti and Ni systems. As experimentally observed in these systems, we approximate this variation of  $T_b$  versus  $\rho$  as a linear one given by

$$T_b(\rho) = T_b(\rho_s) - g \left( 1 - \frac{\rho}{\rho_s} \right) \quad (21)$$

where  $g$  is the slope of the straight line.

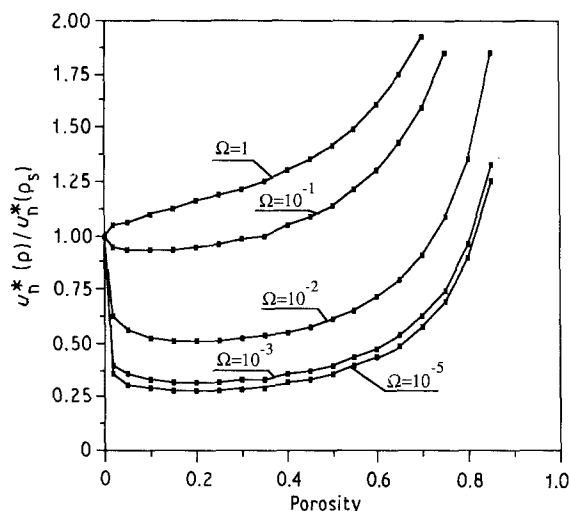


Figure 4 Effect of porosity on the combustion velocity at various values of  $\Omega$ . The combustion velocity has been normalized with respect to the velocity at zero porosity.

In the absence of any particle size effect, we see here a similar trend to that of the overall thermal conductivity, although now the effect of density on the combustion velocity also starts playing a role. Decreasing combustion velocity with decreasing density or increasing porosity has been experimentally observed by various authors [12, 13] although in their observations, as the density decreases beyond some level, the combustion velocity is seen to decrease. This is possibly due to a changing of phases with combustion temperature level, and the present formulation does not consider this effect. At very high porosity, when we can consider the powder to be more or less loosely packed, the combustion velocity increases dramatically. To the author's knowledge experimental combustion synthesis study has not been made at such a high porosity level, where it will be extremely difficult to maintain compact integrity. It might well be that the present modelling breaks down for such a high porosity, since in this case there can be large geometrical changes in the continuum while reaction is in progress, thus changing the heat transfer balance. Further experimental work will be helpful to verify such theoretical predictions at high porosity levels.

We now look at the effect of radiation inside the pores on the overall combustion velocity, as shown in Fig. 5. For a constant pore size, the model predicts that the combustion velocity increases as the porosity level decreases. This is quite expected, since by maintaining a constant radiation effect in the pores at low pore sizes, decreased porosity enhances the local conduction process and hence it gives rise to the enhancement of combustion velocity. One observes, however, an interesting crossover pattern for larger pore sizes (approximately for  $\Omega > 1.25 \times 10^{-1}$ ). In this regime the combustion velocity is decreased by reducing the porosity for a given pore size. It is expected that at such a large pore size, the radiation process becomes more dominant over the local conduction, since increasing porosity at a fixed pore size will necessitate increasing the number of pores and thus the total radiation effect will increase. This correlates with our earlier observation in Fig. 3 that

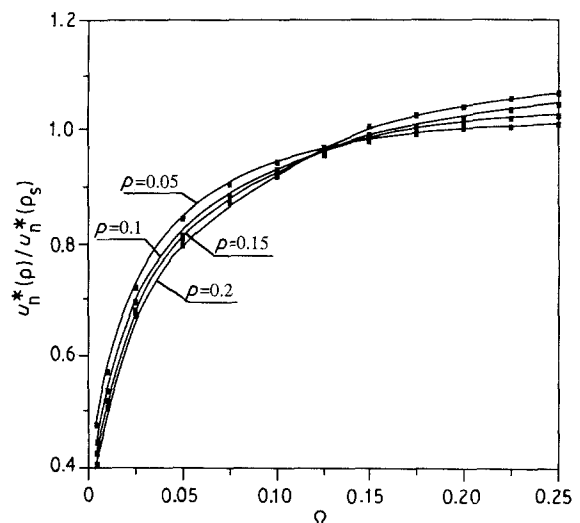


Figure 5 Radiation contribution to the normalized combustion velocity at various levels of porosity;  $\Omega = 4\nu \varepsilon \sigma T_b^3(\rho_s)/k_s$ .

for very large pore size, the effective conductivity will continue to increase with increasing porosity due to an increasing contribution from radiation inside the pores. However, in reality the powder compaction will usually give rise to pore sizes in the range of  $\Omega < 10^{-2}$  and hence the observation that combustion velocity continuously increases with decreasing porosity is valid for such cases.

### 3.2. Effects of particle size

Fig. 6 shows the variation of average particle diameter  $d$  and pore size  $v$  with changing porosity  $p$  at a fixed compaction pressure  $P$  as given by Equation 10. Given the initial state of a compact, this plot can be used deterministically if one of the above three variables is known at a final stage, and this should hold for any applied pressure. For looking at the effect of particle size on the combustion process, let us take specific examples where we consider a few compacts made under a sufficiently high constant applied pressure as shown in Table II. Let us also consider that the compact D is the reference case for the purpose of normalization to obtain non-dimensional results.

As discussed in Section 2, compacts having a higher particle size will have a lower porosity level under the same applied pressure and will have a higher porosity level with lower particle size. Fig. 7 represents a typical plot of normalized combustion velocity varying with normalized particle size. In the absence of any known instances of porosity changing with particle size for the present system, we consider some hypothetical porosity levels for compacts having different particle sizes as shown in Table II. This is simply to

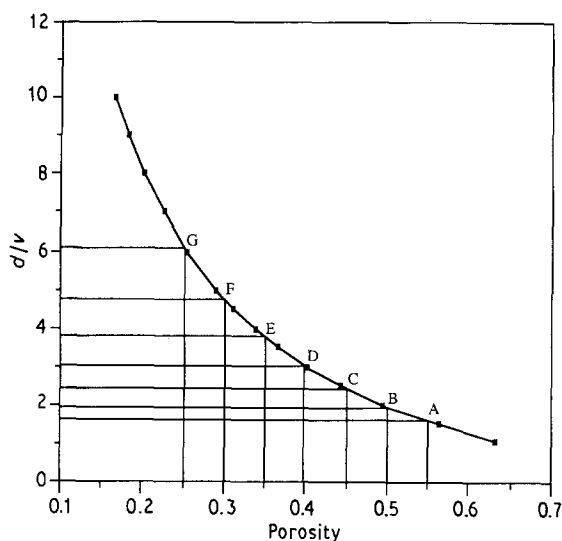


Figure 6 Relationship between porosity, pore size and particle size under a constant applied pressure  $P$ .

TABLE II Variation of porosity level with particle size

| Compact No.                         | A    | B    | C    | D   | E    | F   | G    |
|-------------------------------------|------|------|------|-----|------|-----|------|
| Particle diameter ( $\mu\text{m}$ ) | 2.5  | 6.25 | 12.5 | 25  | 50   | 125 | 250  |
| Porosity                            | 0.55 | 0.5  | 0.45 | 0.4 | 0.35 | 0.3 | 0.25 |

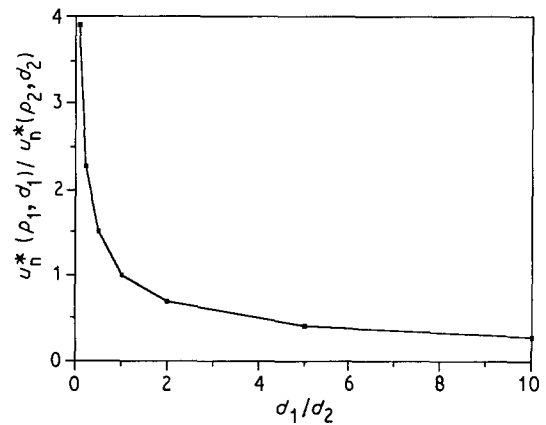


Figure 7 Predicted combustion velocity for different particle sizes, normalized with respect to particle size of  $25 \mu\text{m}$  and porosity 40%.

illustrate the predictability of the present model, but in an actual situation precise measurement of porosity can be conveniently done through microscopic or non-destructive evaluation and should be used for actual calculation.

The compacts as designated in Table II are also indicated in Fig. 6 so that one can directly obtain  $d/v$  ratios for the respective porosity levels. From these values the pore size parameter  $\Omega$  can be obtained. We use Equation 21 for evaluating this parameter, and we also note that the adiabatic combustion temperature  $T_b(\rho_s)$  is known for the system. The velocity ratio plotted in Fig. 7 is seen to decrease continuously with an increase in particle size. The rate of decrease for the smaller particle sizes is very quick and it gradually tends to slow down for larger particle sizes. Very similar behaviour in combustion wave propagation has been observed by Azatyan *et al.* [12] for the titanium-silicon system.

It must be pointed out, however, that in reality the combustion process in a system will be more complex than has been considered here, since at present the combustion-front temperature has been empirically made dependent on porosity from experimental observations. What has not been considered in the present analysis is its kinetic dependence on the particle size. Also, a change in combustion temperature is expected to directly affect the phases that are formed, which in turn may relate to substantially different heats of formation, activation energy etc. and thus the whole transfer process may be affected.

## 4. Conclusions

An attempt has been made here to approximately model the steady-state reaction propagation behaviour in gasless exothermic reactions. The propagation rate is modelled as a function of green compact porosity, pore size and particle size and then respective roles are evaluated quantitatively. The model is based on the concept of an overall local thermal conductivity of a porous compact and the compact has been modelled as a regular array of unit cells of characteristic pore size and spacing related to the porosity. A kinetic function of the heterogeneous reaction rate for describing the reaction in terms of transformed and

untransformed parts of reactant particles has been assumed to be locally applicable to the porous medium in a thermal sense.

It is found that the steady-state wave propagation rate increases with decreasing porosity. Also, as the pore size becomes bigger the radiation effect inside the pores becomes important because the distance through which radiation can propagate becomes larger, and this phenomenon gives rise to an increasing propagation rate for the combustion reaction with increasing pore size. As experimentally observed, the model also correctly predicts that the combustion rate considerably decreases with increasing particle size. This happens because the rate of heat release in the system is reduced due to increase in the reactant contact area, so that the intensity of the ignition process is reduced.

## References

1. A. G. MERZHANOV and I. P. BOROVINSKAYA, *Dokl. Akad. Nauk SSSR* (English translation) **204** (1972) 429.
2. N. P. NOVIKOV, I. P. BOROVINSKAYA and A. G. MERZHANOV, in "Combustion Process in Chemical Technology and Metallurgy", edited by A. G. Merzhanov (Akad. Nauk SSSR, USSR, 1975).
3. B. V. NOVOZHILOV, *Dokl. Acad. Sci. USSR, Phys. Chem.* (English translation) **141** (1961) 151.
4. O. R. BERGMAN and J. BARRINGTON, *J. Amer. Ceram. Soc.* **49** (1966) 502.
5. A. G. MERZHANOV, G. G. KARYUK, I. P. BOROVINSKAYA, S. Y. SHARIVKER, E. I. MOSHKOVSKII, V. K. PROKUDINA and E. G. DYAND'KO, *Sov. Powder Metall. Met. Ceram.* (English translation) **266** (1981) 709.
6. B. MANLEY, J. B. HOLT and Z. A. MUNIR, in "Sintering and Heterogeneous Catalysis", *Materials Scientific Research* Vol. 16 (1984) p. 303.
7. Z. A. MUNIR, *Amer. Ceram. Soc. Bull.* **67** (1988) 342.
8. W. L. FRANKHAUSER, K. W. BRENDLY, M. C. KIESEZEK and S. T. SULLIVAN, "Gasless Combustion Synthesis of Refractory Compounds" (Noyes Publications, New Jersey, 1985).
9. A. P. HARDT and P. V. PHUNG, *Combust. Flame* **21** (1973) 77.
10. B. I. KHACHIN and A. G. MERZHANOV, *Combust. Explos. Shock Wave* **2** (3) (1966) 22.
11. B. V. NOVOZHILOV, *Dokl. Akad. Nauk SSSR* **144** (1962) 1328.
12. T. S. AZATYAN, V. M. MAL'TSEV, A. G. MERZHANOV and V. A. SELEZNEV, *Combust. Explos. Shock Wave* **15** (1979) 35.
13. R. W. RICE, G. Y. RICHARDSON, J. M. KUNETZ, T. SCHROETER and W. J. McDONOUGH, *Ceram. Engng Sci. Proc.* **7** (1986) 736.
14. D. A. ZUMBRUNNEN, R. VISKANTA and F. P. INCROPERA, *Int. J. Heat Mass Transfer* **29** (1986) 275.
15. A. V. LUIKOV, A. G. SHASHKOV, L. L. VASILIEV and Y. E. FRAIMAN, *ibid.* **11** (1968) 117.
16. A. K. BHATTACHARYA, *J. Amer. Cer. Soc.* **74**(9) (1991) 2113.
17. H. H. HAUSNER (ed.), "Modern Developments in Powder Metallurgy" (Plenum Press, New York, 1966) p. 183.
18. A. G. MERZHANOV and B. I. KHAIKIN, *Progr. Energy Combust. Sci.* **14** (1988) 1.
19. Y. C. YI and J. J. MOORE, *J. Mater. Sci.* **25** (1990) 1159.
20. J. B. HOLT and Z. A. MUNIR, *ibid.* **21** (1986) 251.
21. A. K. BHATTACHARYA, Unpublished work (1990).
22. V. P. STOVBUN, V. V. BARZYKIN and K. G. SHKADINSKII, *Combust. Explos. Shock Wave* **13** (1977) 121.
23. S. D. DUNMEAD, D. W. READEY, C. S. SEMLER and J. B. HOLT, *J. Amer. Ceram. Soc.* **72** (1989) 2318.
24. T. TAKAHASHI and T. KIKUCHI, *J. Nucl. Mater.* **91** (1980) 93.

Received 7 November 1990  
and accepted 10 April 1991